Experimental evidence for the effect of hydrographs on sediment pulse dynamics in gravel-bedded rivers

Robert Humphries,[1,2] Jeremy G. Venditti,[1] Leonard S. Sklar,[2] and John K. Wooster[3]

Received 17 January 2011; revised 17 November 2011; accepted 22 November 2011; published 21 January 2012.

[1] Gravel augmentation is a river restoration technique applied to channels downstream of dams where size-selective transport and lack of gravel resupply have created armored, relatively immobile channel beds. Augmentation sediment pulses rely on flow releases to move the material downstream and create conditions conducive to salmon spawning and rearing. Yet how sediment pulses respond to flow releases is often unknown. Here we explore how three types of dam releases (constant flow, small hydrograph, and large hydrograph) impact sediment transport and pulse behavior (translation and dispersion) in a channel with forced bar-pool morphology. We use the term sediment "pulse" generically to refer to the sediment introduced to the channel, the zone of pronounced bed material transport that it causes, and the sediment wave that may form in the channel from the additional sediment supply, which can include input sediment and bed material. In our experiments, we held the volume of water released constant, which is equivalent to holding the cost of purchasing a water volume constant in a stream restoration project. The sediment pulses had the same grain size as the bed material in the channel. We found that a constant flow 60% greater than the discharge required to initiate sediment motion caused a mixture of translation and dispersion of the sediment pulse. A broad crested hydrograph with a peak flow 2.5 times the discharge required for entrainment caused pulse dispersion, while a more peaked hydrograph >3 times the entrainment threshold discharge caused pulse dispersion with some translation. The hydrographs produced a well-defined clockwise hysteresis effecting sediment transport, as is often observed for fine-sediment transport and transport-limited gravel bed rivers. The results imply a rational basis for design of water releases associated with gravel augmentation that is directly linked to the desired sediment behavior.

Citation: Humphries, R., J. G. Venditti, L. S. Sklar, and J. K. Wooster (2012), Experimental evidence for the effect of hydrographs on sediment pulse dynamics in gravel-bedded rivers, *Water Resour. Res.*, *48*, W01533, doi:10.1029/2011WR010419.

1. Introduction

[2] Dams provide flood control, fresh water supply, debris retention, and hydroelectric power, but they also restrict coarse sediment supply to downstream reaches [*Ligon et al.*, 1995]. This lack of sediment supply can cause riverbeds to incise, coarsen and become immobile, making them unsuitable spawning and rearing habitat [*Kondolf*, 1997; *Buffington and Montgomery*, 1999]. Gravel augmentation is a stream restoration tool that involves the addition of gravel to a system depleted of its coarse sediment supply downstream of a dam. The goal is to rejuvenate salmonid spawning habitat and restore geomorphic activity [*Bunte*, 2004; *Pasternack et al.*, 2004; *Harvey et al.*, 2005]. Passive gravel augmentation is a popular restoration strategy in which a volume of gravel is placed in the channel, or on a riverbank, with the expectation that high flows will distribute the gravel downstream, depositing it in morphologies suitable for spawning habitat [*Bunte*, 2004]. However, the outcome of adding sediment is difficult to predict and usually involves a high degree of uncertainty in real rivers [e.g., *Wohl et al.*, 2005]. Postproject monitoring, although rare, often reveals that projects have performed poorly, with limited habitat restoration benefits [*Kondolf*, 1997; *Lutrick*, 2001]. This has prompted a series of investigations designed to identify the most effective method of distributing added gravel using physical laboratory modeling techniques [cf. *Sklar et al.*, 2009; *Venditti et al.*, 2010a, 2010b].

[3] Passive gravel augmentation creates a pulsed sediment supply to a channel, similar to natural sediment pulses created by landslides, debris flows and other sources of episodic sediment supply. We use the term "pulse" generically to indicate a body of sediment introduced to a channel, the zone of pronounced bed material transport that it causes and the sediment wave that may form in the channel from the additional sediment supply, which can include input sediment and bed material. Natural sediment pulses have received considerable attention in the literature and investigations have included field studies [*Gilbert*, 1917; *Madej*, 2001; *Sutherland et al.*, 2002; *Kasai et al.*, 2004; *Bartley and Rutherford*, 2005; *Hoffman and Gabet*, 2007],

[1]Department of Geography, Simon Fraser University, Burnaby, British Columbia, Canada.
[2]Department of Geosciences, San Francisco State University, San Francisco, California, USA.
[3]Fisheries Division, NOAA, Sacramento, California, USA.

0043-1397/12/2011WR010419

flume experiments [*Lisle et al.*, 1997; *Cui et al.*, 2003a; *Sklar et al.*, 2009; *Venditti et al.*, 2010a, 2010b] and numerical modeling [*Pickup et al.*, 1983; *Benda and Dunne*, 1997a, 1997b; *Lisle et al.*, 2001; *Cui et al.*, 2003b; *Cui and Parker*, 2005; *Cui et al.*, 2008]. These studies have shown that sediment pulses move by some combination of dispersion or translation, but that dispersion is by far the dominant progression pattern [*Lisle et al.*, 1997; *Cui et al.*, 2003b; *Lisle*, 2008]. A recent synthesis by *Lisle* [2008] has shown that low-amplitude sediment waves and pulses that are finer than the bed material are more likely exhibit some translation, in addition to dispersion.

[4] There has been relatively little work done on sediment pulses in channels without an upstream sediment supply, as occurs downstream of a dam. It is reasonable to assume that an upstream sediment supply increases the likelihood of dispersion and decreases the likelihood of any translation. Recent work by *Sklar et al.* [2009] has begun to address this issue by examining pulse behavior in channels with no sediment supply. They demonstrated that while pulses often exhibit dispersive behavior, pulse grain size and volume play an important role in whether a pulse will display translational behavior. In agreement with the synthesis of *Lisle* [2008], they show small volume pulses and pulses composed of the fine tail of the bed material grain size distribution show a greater tendency for translational behavior. The experimental work undertaken to date has examined pulse movement in simple rectangular shaped channels. The impacts of complex channel topography or variable flow on pulse behavior remain poorly understood. Here we examine how hydrograph shape and forced alternate bar morphology influences pulse dynamics.

[5] There has been some previous work on the impact of hydrographs on sediment transport rates in experimental channels with a constant sediment supply rate [cf. *Bell and Sutherland*, 1983; *Phillips and Sutherland*, 1989, 1990; *Lee et al.*, 2004; *Wong and Parker*, 2006a; *Parker et al.*, 2007]. This work demonstrates that hydrographs do not impact the total volume of sediment transported, relative to a constant flow. The later work [*Wong and Parker*, 2006a; *Parker et al.*, 2007] also suggests that beyond a short reach near the sediment input location, bed sediment texture and elevation are invariant to the fluctuations in flow. The conditions envisioned in the previous work are significantly different than those downstream of a dam where there is no significant sediment supply and water releases are often infrequent and smaller than typical flood flows prior to dam closure. Bed surface texture adjusts to sediment supply [*Dietrich et al.*, 1989; *Buffington et al.*, 1992; *Buffington and Montgomery*, 1999], so periodically adding sediment pulses to a sediment-starved channel along with periodic water releases could impact sediment dynamics in ways not predicted from the previous work. Indeed, the nonlinear relation between shear stress and sediment transport suggests that varying the release hydrograph for a specified volume of water could result in different transport rates and different patterns of transport, in the absence of a constant sediment supply. How this extra transport capacity influences the progression of a gravel augmentation pulse is unknown.

[6] Here we examine the movement of a series of sediment pulses through a gravel-bedded flume channel with well-developed alternate bar topography to expand upon the work of *Sklar et al.* [2009]. We are interested in how a volume of water, delivered to the channel as a constant flow, a small hydrograph, and a large hydrograph impact the movement of a sediment pulse whose grain size is the same as the bed material.

2. Methods

2.1. Flume and Bed Configuration

[7] Experiments were conducted in the 28 m long, 0.86 m wide, and 0.86 m deep sediment feed flume at the Richmond field station (RFS), University of California, Berkeley. The flume is equipped with a computer-controlled instrument carriage, with a laser distance meter and an ultrasonic transducer for measuring bed and water surface topography, respectively. Sediment is supplied at the upstream end by motor-driven auger feeders or by hand, and bed load flux at the downstream end is measured with a tipping bucket suspended from a load cell (see *Venditti et al.* [2010a] for further information).

[8] The bed material was a sediment mixture with a log-normal distribution, a median diameter (D_{50}) of 4.1 mm and a standard deviation of 1.9 mm. The sediment is "moderately sorted" according to the *Folk and Ward* [1957] classification. Approximately 20% of the material was finer than 2 mm (Figure 1). Although the bed sediment distribution straddles the division between sand and gravel, the distribution is unimodal.

[9] To force strongly multidimensional flow, and to encourage sediment scour and deposition patterns that mimic a natural river, we placed sand bags and cobbles in the flume to form six forced bars, spaced 5 channel widths apart (Figure 2). Because the bars were intended to remain immobile, we reinforced the upstream ends with epoxy to

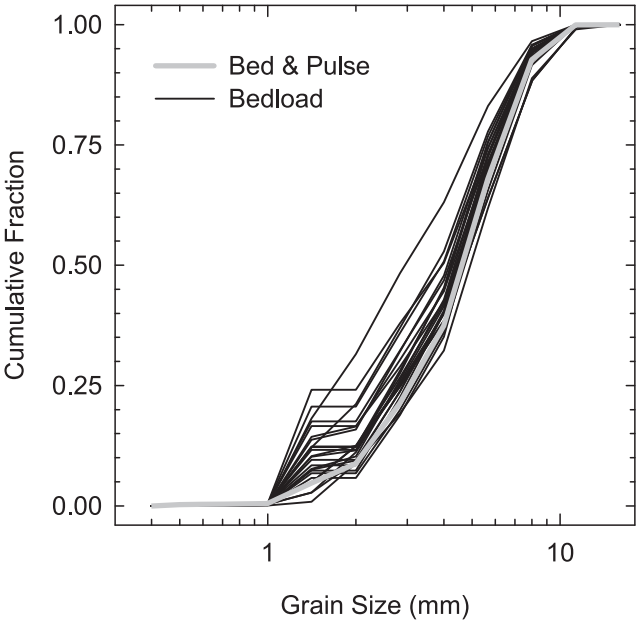

Figure 1. Grain size distributions of the bed material (thick line) and transported material during the pulse runs. The pulses had the same grain size distributions as the bed material.

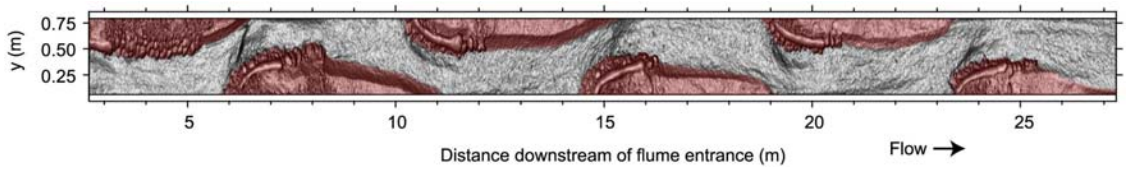

Figure 2. Shaded relief map of bed topography and channel bars. The bars are highlighted red.

withstand the highest discharges imposed. The resulting bed topography consisted of alternating pool and riffle sequences with vertical topographic variations of ~50 mm along the thalweg (Figure 2).

2.2. Experimental Design and Procedure

[10] The experiments were designed to explore the influence of variable flow on the movement of a discrete pulse of sediment introduced over a short period at the upstream end of the flume. This study builds on a previous set of experiments with the same bed configuration, in which pulse volume and grain size were varied but discharge was held constant throughout [*Cui et al.*, 2008]. Here we test the effect of varying the distribution of discharge in time on pulse dynamics, while keeping the total volume of water discharged constant.

[11] We used three discharge patterns in our experiments: (1) a constant flow, (2) a small hydrograph, and (3) a large hydrograph (Figure 3). We designed the hydrographs using a lognormal distribution of discharge over time:

$$Q_w = \frac{C}{\sqrt{2\pi\sigma^2}} e^{-\frac{(T-\bar{T})^2}{2\sigma^2}}, \quad (1)$$

where $T = \log_{10}(\text{time})$, $\bar{T}$ and σ are the log-transformed mean and standard deviation of the distribution of time, respectively, and the coefficient C controls the discharge magnitude. We adjusted C and σ to achieve the desired range of peak discharges while maintaining a constant total volume of water over the 15 h duration. This water volume is the same as the volume of water released during our constant flow over 15 h. Keeping the total water volume of the hydrograph constant, relative to the volume of water used during the constant rate experiments is equivalent to holding the cost of purchasing water constant, for each discharge pattern. For both hydrographs, we kept the time to the peak discharge at 2.5 h from the start of the run. During the experiments, we controlled discharge to follow the design hydrographs by manually adjusting pump speed every 15 min using a variable frequency inverter, and monitored discharge with an acoustic transit time flowmeter installed on the water supply pipe.

[12] Our flow conditions were chosen with reference to the threshold of motion for the bed sediment which we determined by incrementally increasing flow until the first grains moved out of control patches of sediment. This occurred at $Q_{thresh} = 0.011$ m^3 s^{-1}. The constant flow (0.018 m^3 s^{-1}) corresponds to a condition that is ~60% greater than the discharge required to begin entrainment of the bed material. The peak value of the large hydrograph (35 L s^{-1}) corresponds to a bankfull flow where the bar tops are slightly submerged. The peak value of the small hydrograph (25 L s^{-1}) is an intermediate step between the peak of the large hydrograph and constant rate experiments (Figure 3). This corresponds to a flow intermediate between the flow required to initiate sediment movement and the bankfull condition.

[13] We confined our runs to portions of the design hydrographs where $Q_w > Q_{thresh}$ and the shear stress was capable of moving the finest bed material. Hence, the beginning and end of each hydrograph was truncated, giving the small hydrograph a total run time of 14.5 h, and the large hydrograph a total run time of 8.5 h (Figure 3 and Table 1).

[14] For each of the three flow distributions (constant, large and small hydrographs), we performed a sequence of

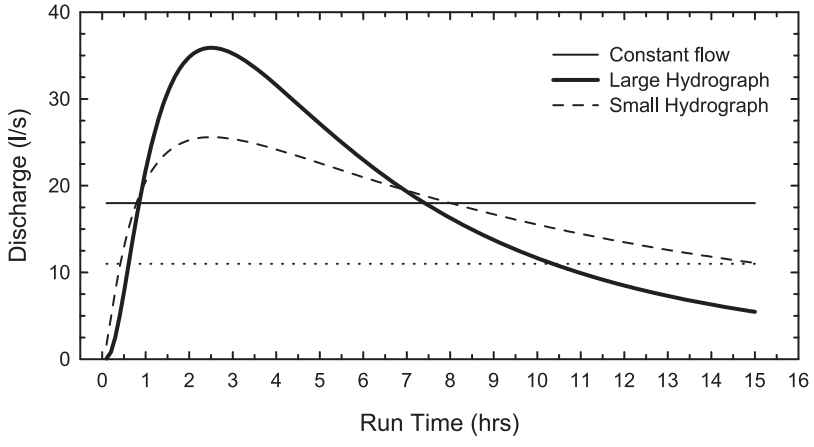

Figure 3. Design discharge distributions for the three flows used. The horizontal dotted line is the threshold of motion for the bed sediment. At the end of each hydrograph, the discharge dropped to zero.

Table 1. Run Sequence, Water Discharge, and Sediment Flux

Run	Hydrograph	Type	Mean Slope ($\times 10^{-3}$)	Duration (h)	Peak Flow (L s^{-1})	Peak Flux (g s^{-1})	Mean Flux (g s^{-1})	Effective Mean Flux[a] (g s^{-1})	Input Mass (kg)	Output Mass (kg)	Lag[b] (h)
C3	constant	armor	9.5	66.0	18.0	n/a	n/a	n/a	0	n/a	n/a
C4	constant	pulse/wash	7.9	34.0	18.0	7.9	1.5	1.5	167	191.9	n/a
S13	large	armor	7.2	10.5	34.8	24.3	5.1	12.7	0	191.1	1.1
S14	small	pulse	7.6	14.5	27.0	3.5	0.5	1.6	167	23.9	0.5
S15	small	wash	7.3	14.5	26.8	6.5	0.9	3.1	0	46.8	−0.8
S16	small	wash	7.3	14.5	25.7	6.1	0.9	3.1	0	46.7	−0.7
L17	large	armor	7.2	8.5	34.5	15.8	3.1	7.2	0	107.7	−0.5
L18	large	pulse	7.0	8.5	35.7	20.0	3.2	9.5	167	141.9	1.4
L19	large	wash	6.1	8.7	35.4	16.3	3.9	8.3	0	123.9	−2.3

[a]Hydrograph runs were truncated when $Q_w < 11$ L s^{-1} (our observed threshold for sediment entrainment); effective duration of all hydrographs was 15 h.
[b]Negative lag means sediment flux peak precedes discharge peak, and positive lag means sediment flux peak comes after discharge peak.

three types of runs (denoted armor, pulse, and wash in Table 1). Armor runs were conducted with no sediment feed, and were intended to develop a relatively low mobility, incised bed with sorting patterns through the bars consistent with hydrograph flows to serve as an initial condition. This channel is analogous to degraded channels downstream of dams. During pulse runs the sediment pulse was introduced to the channel. During wash runs the sediment pulse moved through the channel without any additional sediment supply.

[15] The constant flow experiment was preceded by a run in which we allowed the bed to adjust to a sediment supply of 11.1 g s^{-1}. This run continued until the net aggradation and degradation within the flume became minimal. The constant flow armoring run that followed this phase continued for 66 h (run C3), until the change in bed elevation became minimal. This resulted in significant channel degradation, a decline in mean bed slope from 0.0095 to 0.0079, and bed surface coarsening, but preserved the pool-riffle sequences, forming a series of terraced bars (Figure 2). There was sediment transport at the end of the armoring run, but it was 14% of the original sediment feed, which translated to 0.05 mm h^{-1} of topographic change over the entire flume.

[16] For the hydrograph runs, it was necessary to establish the same degraded, armored bed that was developed for the constant flow pulse. However, it would have been inappropriate to use a constant flow to set this as the initial condition because the hydrograph causes a transient period of sediment motion that can influence bed texture. As such, the first hydrograph in both sequences (small and large) was run without a sediment supply to create a degraded, armored bed with texture patterns consistent with the bar topography and a hydrograph. We chose a large hydrograph to set this initial condition for both the small and large hydrograph sequences such that the initial conditions would be comparable. There was sediment transport at the peak of the hydrograph armoring runs (Table 1).

[17] Sediment pulses were introduced following the armoring runs. Each pulse was identical in terms of grain size distribution, total mass input, delivery rate and method of introduction to the channel. The sediment pulses were composed of the same grain size distribution as the original bed material used to develop the channel, differing only in that we painted and dried the pulse sediment in a cement mixer. The mass of each pulse (167 kg) was scaled to the amount required to cover the bed of the entire flume one bed material D_{50} deep in the loosest possible packing. Gravel augmentations in natural channels are often intended to bury the existing bed material and our pulse scaling satisfies that design. We fed each sediment pulse into the flume at 43.5 g s^{-1} over 64 min at the apex of the farthest upstream bar ~3 m downstream of the channel entrance (Figure 2).

[18] The first sediment pulse was introduced at the beginning of the constant flow run (run C4).

[19] The second sediment pulse was introduced during the rising limb of the first of three small hydrographs (runs S14, S15, and S16). The third sediment pulse was introduced during the rising limb of the first of two large hydrographs (L18 and L19).

[20] During each run, we monitored the pulse movement in the flume, its effect on bed and water surface topography, as well as the transport rate and grain size of bed load material exiting the flume. We were able to track the sediment pulse movement because it was a different color than the bed material. At each 15 min interval of the hydrographs, the water surface profiles, spaced at 60 mm intervals across the flume width, were measured every 5 mm along the flume length using an ultrasonic transducer mounted to the computer-controlled cart that traversed the length of the flume. The transducer has a practical resolution (based on its calibration) of ±1 mm. Bed load was monitored using a continuous weighing mechanism that recorded the weight of material leaving the flume at 10 s intervals. Each hydrograph was conducted in four stages and the flow was stopped at 2, 4, 6, and 15 h of runtime during which we removed and sieved the sediment in the bed load collection mechanism and photographed the bed surface. We also measured bed topography on a 10 × 10 mm grid using the laser distance meter attached to the computer controlled cart. The laser is accurate to ±0.1 mm, which is smaller than the finest grains in the flume. The practical resolution of the laser scan is the size of the smallest grains in the flume or ~1 mm.

2.3. Sediment Flux Estimation

[21] To compare sediment flux during the constant and hydrograph flows condition, we estimated bed load transport rate using three techniques: (1) integration of the measured bed load from the sediment trap at the downstream end of the flume, (2) volumetric calculation of sediment eroded from the flume using net change between the high-resolution topographic surveys, and (3) the sediment transport capacity equation of *Wong and Parker* [2006b] integrated over time. We approached the sediment flux

calculations in these three different ways because they highlight different aspects of what is happening in the channel. The measured sediment flux gives us the total material exiting the channel. The volumetric sediment transport rate should be the same as the measured sediment flux unless pulse material is stored in the flume or there is sediment eroded from outside our topographic surveys (e.g., from the bar tails). Comparison of the measured and predicted sediment flux highlights gaps in our ability to model sediment transport through channels with the standard model.

[22] In order to calculate the total measured sediment flux (Q_{s-meas}), we simply sum the total amount of material collected by the bed load collection mechanism at the end of the flume during each discharge pattern and divide it by the total run time. The bed load measurement system reports the submerged weight of sediment in the tipping drum sediment trap at 10 s intervals. The dry mass transport rate is the mass difference between measurements multiplied by 1.6 and divided by the time interval. Minor contamination of the signal occurred when the weighing drum was nearly empty for long periods of time and able to move easily in the end tank because of turbulence. With $\sim$1 kg of sediment in the collection drum, this contamination disappears. There were also periods of high-frequency signal dropouts. To deal with these problems, we reconstructed the signal using the maximum cumulative sediment flux recorded over a 300 s window. The difference between the raw and reconstructed cumulative flux over a full hydrograph is $<$2% for both 60 s and 300 s windows, suggesting the bias introduced in the signal processing was minor.

[23] We used the laser surveys of the flume bed to estimate the mean sediment flux (Q_{s-vol}) over the time interval between scans (dt) by differencing the surveyed surfaces, such that

$$Q_{s-vol} = \frac{\rho_s \, dV \, (1-\lambda) + M_{pulse}}{dt}, \tag{2}$$

where dV is the change in the volume of sediment in the flume, ρ_s is the sediment density (2650 kg m^{-3}), λ is the bed porosity (40% [*Wooster et al.*, 2008]), M_{pulse} is the mass of pulse sediment input to the flume ($M_{pulse} = 0$ except for the first time intervals of runs C4, S14 and L18). We explicitly assume the sediment transport into our measurement area is negligible.

[24] To estimate the sediment transport capacity as a function of the varying discharge we used the relation of *Wong and Parker* [2006] because it is based on flume measurements for the range of sediment sizes used in our experiments. The predicted sediment mass flux is given as

$$Q_{s-WP} = \rho_s W \sqrt{rgD_{50}^3} 4.93 (\tau^* - \tau^*_{crit})^{1.6}, \tag{3}$$

where τ^* is the nondimensional shear stress

$$\tau^* \equiv \frac{\tau_b}{(\rho_s - \rho_w) g D_{50}} = f_b \frac{hS}{rD_{50}}, \tag{4}$$

[25] τ_b is the shear stress acting on the bed sediments, D_{50} is the median diameter of the bed material, ρ_s and ρ_w are the densities of the sediment and fluid, respectively, g is gravitational acceleration, h is the flow depth, W is the wetted channel width, S is the channel slope, f_b is the fraction of the total boundary shear stress available to transport bed sediment, and $r = (\rho_s - \rho_w)/\rho_w = 1.65$. In the *Wong and Parker* [2006] relation, the critical nondimensional shear stress for sediment entrainment (τ^*_{crit}) is set to 0.047. Our observed threshold of $Q_{thresh} = 0.011$ m^3 s^{-1} is equivalent to $\tau^* = 0.046$.

[26] To estimate the depth-slope product shear stress as a function of discharge we fit power functions to measured values of reach-averaged flow depth and water surface slope obtained from the ultrasonic and laser scans. Following the methods outlined by *Cui et al.* [2008], we calculated reach-averaged flow depth as the difference between the cross-stream-averaged water surface and mean bed surface elevation excluding portions of the topography that extend above the water surface. To avoid effects of boundary conditions we also excluded the bed and water surface topography within 3 m of both the entrance and exit of the flume. Slope was determined by fitting a linear trend line to the cross-stream averaged water surface topography. As expected, depth varied systematically with discharge. Water surface slope also increased with discharge, presumably because of the reduction in channel confinement with increasing distance downstream. This subtle trend in channel geometry was due to the bed degradation following the initial armoring runs, which reduced the bed slope but did not affect the height or downstream slope of the bar surfaces.

[27] To apply the *Wong and Parker* [2006b] relation (equation (3)) to our flume, we used the constant flow (run C4) sediment flux measurements to calibrate the shear stress partitioning coefficient (f_b), such that the predicted flux matched the observed flux averaged over the 34 h run duration. This was achieved with $f_b = 0.622$, in good agreement with typical values obtained from analysis of field settings of bar-pool topography [e.g., *Andrews*, 2000]. We assume the shear stress partitioning between bed stress and form drag does not change significantly with discharge, and hold f_b constant through the sediment transport calculations reported below.

3. Sediment Flux Response to Constant and Hydrograph Flows

[28] Figure 4 shows the response of sediment flux in the channel to water discharge for the three sediment pulses. During the constant flow (run C4), sediment exited the channel at mean rate of 1.6 g s^{-1} (Figure 4a). The bulk of the pulse material passed through the flume in the first 15 h, with a slight increase in flux rate at hour 10. After hour 15, the material exiting the channel was a mixture of bed material and painted pulse material. Overall the sediment pulse had little impact on sediment flux. Transport rates varied between 0.25 to 5.5 g s^{-1} with a periodicity in variations of 1–3 h (Figure 4a). This variability derives from the way the sediment pulses moved through the bar forms. Sediment tended to accumulate adjacent to the bar apex and at the downstream end of pools. This accumulated sediment was then released from these zones as local sediment waves.

[29] During the hydrograph runs, sediment transport rates varied with the discharge (Figure 4). Peak transport

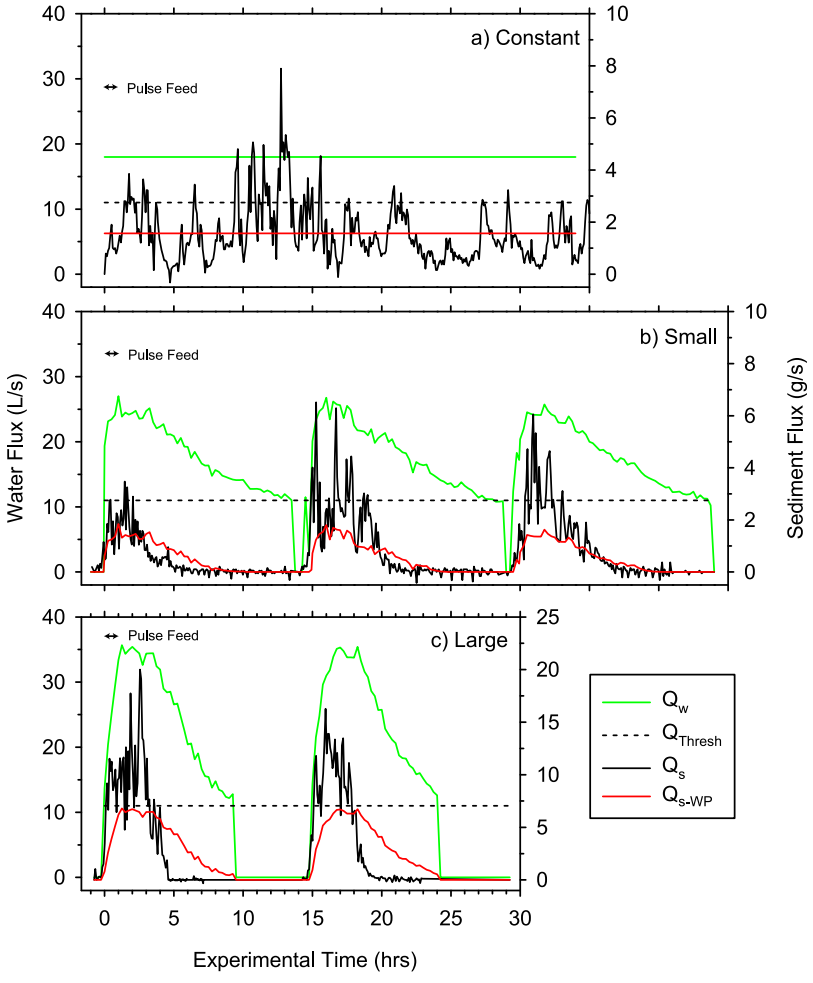

Figure 4. Hydrographs and sedigraphs showing the water supply (Q_w) and sediment flux out of the channel (Q_s) for (a) the constant flow (run C4), (b) the series of three small hydrographs (runs S14, S15, and S16), and (c) the series of two large hydrographs (runs L18 and L19). Run times are set such that t = 0 s is when the sediment pulse feed begins. When the hydrograph curve has a value of zero, flows were below the threshold of motion for sediment in the channel ($Q_{thresh} = 11$ L s^{-1}), and the water supply was stopped. Q_{s-WP} is the sediment flux predicted using equation (3).

rates at the downstream end of the flume lagged behind the peak discharge of the hydrograph in runs where the pulse was added (S14 and L18; Table 1). However, in subsequent runs where the hydrographs were repeated without sediment inputs (runs S15, S16, and L19) sediment flux peaked before the maximum discharge. The lag between the hydrograph peak and the sediment flux peak reflected the time necessary for the pulse to pass through the channel. Bed load grain size also varied with sediment flux, coarsening on the rising limb of hydrographs and fining on the receding limb (Figure 5). The bed load fining on the recession limbs was greater for the large hydrographs than the small hydrographs.

[30] The total sediment mass delivered to the flume exit, for a fixed volume of water supplied, provides a metric for the relative sediment transport efficiency of the different distributions of discharge over time. Figure 6 shows the cumulative sediment flux leaving the flume as a function of time. Cumulative sediment flux is greatest for the large hydrograph, smallest for the small hydrograph, and intermediate between these for the constant flow. For the constant discharge run, the trend in cumulative sediment flux (Q_{s-meas}) is nearly linear, while for the hydrographs, the increases are punctuated with periods where sediment was leaving the channel during peak flows and periods where the cumulative flux did not increase during the declining limbs of the hydrographs.

[31] Over the first 30 h of the constant flow run, 175.7 kg of sediment exited the channel, a mass nearly equal to the sediment pulse mass of 167 kg. After the first 15 h, the large hydrograph (run L18) delivered 141.9 kg to the sediment trap. We do not know the exact proportions of the painted pulse material to the bed material in the bed load, but the volumes suggest most of the sediment pulse had exited the channel or was exchanged with bed material. After 30 h, the large hydrographs delivered 265.7 kg to the sediment trap, which is 59% more than was input. In contrast, the small hydrograph delivered only 23.9 kg during the first 15 h after the pulse injection (run S14). Even after two more small hydrographs passed through the flume

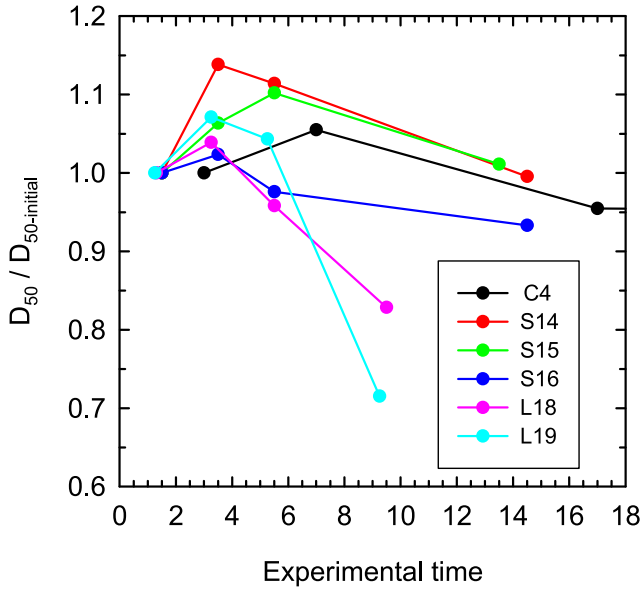

Figure 5. Change in bed load median grain size (D_{50}) normalized by its value at the beginning of the run ($D_{50\text{-initial}}$).

(runs S15 and S16), the cumulative flux amounted to only 117.4 kg, or 70% of the mass of the pulse input.

[32] Cumulative sediment flux estimates using the volumetric differencing of bed surface scans (equation (2)) are similar to the net mass accumulation measured by the sediment trap (Figure 6). However, the volumetric change overestimates transport during the constant and small hydrograph. In equation (2), we added the pulse volume to the volumetric sediment flux, so $Q_{s-vol} > Q_{s-meas}$ suggests that some pulse material is still stored in the channel. Cumulative sediment flux is less than Q_{s-meas} during the large hydrographs, suggesting that the pulse material had left the flume and sediment was excavated from outside our topographic survey area, specifically the bar tails.

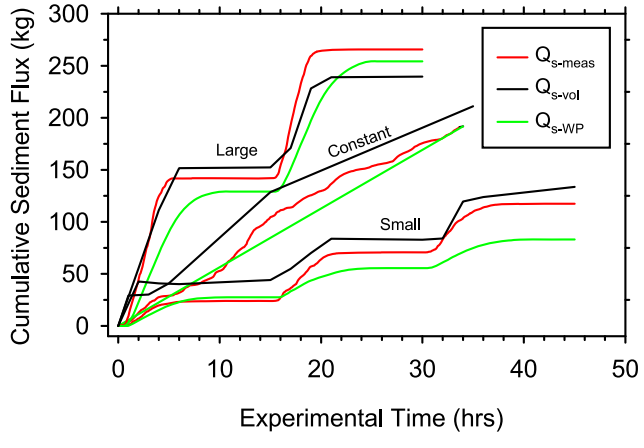

Figure 6. Cumulative sediment flux for constant flow, small hydrograph, and large hydrograph runs. Sediment flux is calculated from the instantaneous measurements (Q_{s-meas}), the observed change of sediment volume in the flume (Q_{s-vol}), and the *Wong and Parker* [2006b] equation (Q_{s-WP}).

[33] Comparison of measured sediment flux with predicted sediment transport capacity (equation (3)) shows good agreement for the cumulative flux produced by the large hydrograph, but the model underpredicts measured flux for the small hydrographs by 29% (Figure 6). A minor adjustment of our form drag coefficient (f_b) to 0.636 (from 0.622) for the small hydrographs would match the predicted sediment flux magnitude to the observed.

[34] Comparison of the sediment flux magnitude masks a more substantial divergence between the predicted and observed sedigraphs. The model reproduces the pattern of sediment discharge for the small hydrograph, but not for the large hydrograph (Figure 4). The model predictions roughly match the observed flux on the rising limb and at the peak discharge for both large and small hydrographs (Figure 4), however the principal deviation between model and observed flux occurs on the recession limb of the large hydrographs. Sediment transport at the downstream end of the flume drops to near zero on the recession limb at a much higher discharge than the threshold discharge of 11 L s^{-1} for the initiation of sediment motion.

[35] The rapid decline in sediment transport rate early in the recession limb leads to a well-defined clockwise hysteresis effect. For example, Figure 7a shows sediment transport rate versus discharge for run L18, the large hydrograph run with the sediment pulse feed. The data are stratified to show the difference in the relation between flow and sediment transport for the rising and falling limbs of the hydrograph. When plotted on a log-log scale (Figure 7b), the hysteresis causes a difference in the slope of the relation between sediment discharge (Q_s) and water discharge (Q_w) for rising and falling limbs of the hydrograph. Increases in Q_s with Q_w are more gradual on the rising limb than on the falling limb of the hydrograph. There is a greater difference between the slopes of the transport relation between the small and large hydrographs (Figure 7c).

[36] The rising limb of the small hydrographs (including the peak) moved 38% of the sediment while the falling limbs transported 62% (Figure 4b). The rising and falling limbs of the large hydrographs each moved half of the sediment transported (Figure 4c). More sediment (small 5% and large 14%) is moved by the first hydrograph rising limb than subsequent hydrographs in a series.

4. Pulse Morphodynamics

4.1. Reach-Scale Pulse Movement

[37] As the leading edge of the pulse progresses through the system, it varies its subreach scale celerity in response to the local flow conditions created by the forced topography. The leading edge of the pulse progressed downstream in an episodic pattern, moving rapidly through the deeper portions, and more slowly through shallower zones, sometimes stalling and aggrading. Figure 8a shows a photograph of the leading edge of the sediment pulse during the first large hydrograph. The pulse material is painted green so that it contrasts against the bed material. Figures 8b and 8c show shaded relief maps of the bed before the first large hydrograph and the topography that corresponds to the photo. A map of the change in elevation between Figures 8b and 8c is shown in Figure 8d.

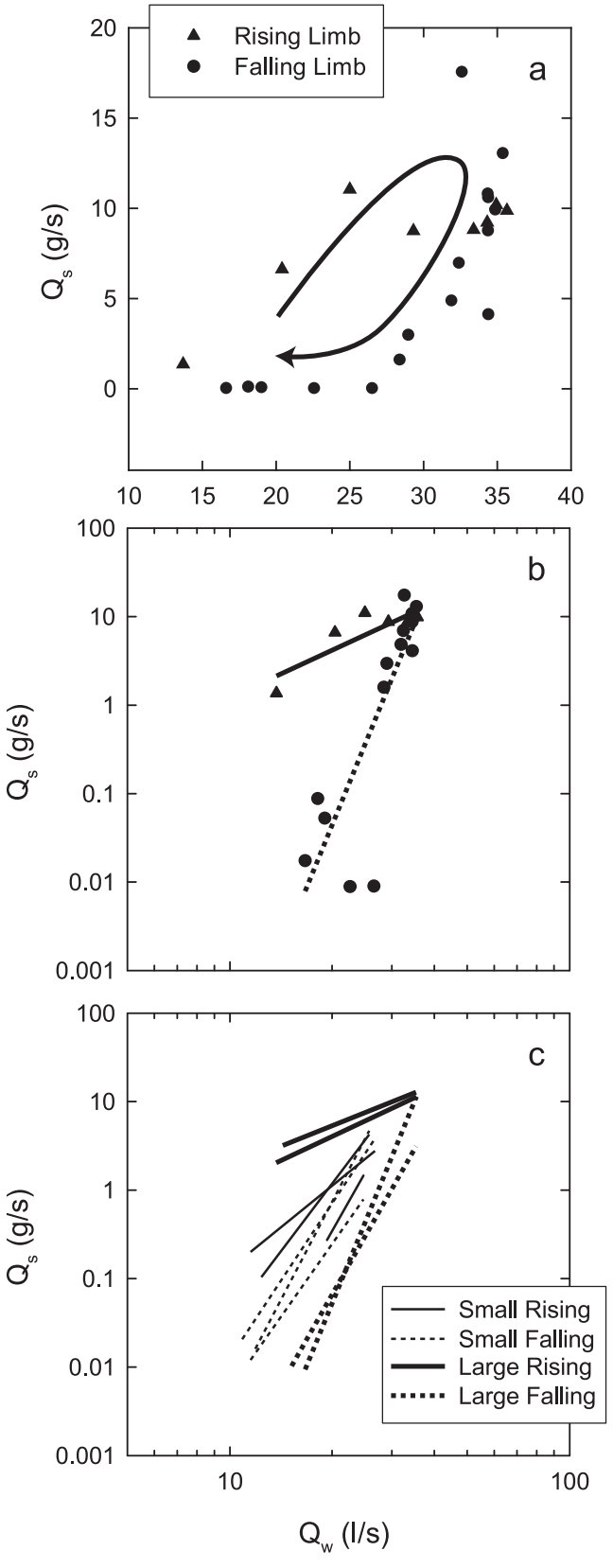

Figure 7. Relation between sediment (Q_s) and water discharge (Q_w). (a and b) Data have been separated to show rising and falling limbs of the hydrograph and the corresponding Q_s during the first large hydrograph. (c) Lines show the linear regressions for all hydrographs.

[38] As the pulse material passes through the pool-riffle topography, the pulse particles first pass through the scour hole that forms adjacent to the forced bar head (scour A in Figure 8e) and begin to distrain, causing local aggradation (stall point A). This aggradation begins with the coarser particles, as they are most likely to distrain, enhancing drag and deposition. As the deposit grows, it deflects the local flow toward the flume wall and forces development of a new scour hole (scour B) adjacent to the flume wall (Figure 8e).

[39] The material removed from scour B was distrained as particles moved downstream into the pool tail out adjacent to the downstream bar head forming a second sediment deposit (stall point B). As this process continues, scour B becomes the primary flow path for material that is entering the upstream pool adjacent to the upstream bar head. This new flow path causes sediment entering the reach to bypass stall point A and the associated deposit ceases to aggrade. scour B ceases to deepen as the new material entering the reach replaces the removed material. Aggradation at stall point B ceases as sediment is passed through downstream scour hole A.

[40] The resulting bed deformation peaked shortly after the leading edge of the pulse bypassed the original deposit (stall point A in Figure 8e), which subsequently degrades. The rest of the pulse material passes through the reach without interacting with the sediment deposit morphology, moving as low-amplitude sheets in the center of the channel. As the bed becomes starved of sediment from upstream, the deposits erode and the channel returns to its previous morphology, often with some minor overall bed lowering.

4.2. Multireach-Scale Pulse Morphodynamics

[41] Figure 9 shows maps of topographic change as the sediment pulse moves through the channel for the constant flow, small hydrograph and large hydrographs. In the constant flow (Figure 9a), the pulse sediment moves downstream from storage element to storage element as described above. The leading edge of the pulse does not travel more than a few bar lengths ahead of the main body of the pulse, but the tailing edge of the pulse remains within the flume for an extended period of time, decaying after the main body of the pulse passed, and finally exits the flume sometime between sampling times 14:42:40 and 34:39:08 (Figure 9a).

[42] Figure 9b indicates that the first small hydrograph was insufficient to move the pulse material to the end of the channel. After the second small hydrograph, the leading edge of the pulse exits the flume while the rest of the pulse remained in the channel, accumulated on the apex of the alternate bars. In light of this observation, a third hydrograph was introduced to the channel that was in addition to the two hydrographs that were equivalent to the water released during the 30 h constant flow run. By the end of the third hydrograph, the tail of the pulse had still not moved downstream and the pulse material had still not exited the flume. The failure of the sediment pulse to exit the channel during the first two hydrographs suggests greater dispersion of the pulse sediment compared to the constant flow run. The addition of the third hydrograph demonstrates the stability of the sediment deposits.

[43] In the large hydrograph experiment, most of the pulse exited the flume during the peak and declining limb

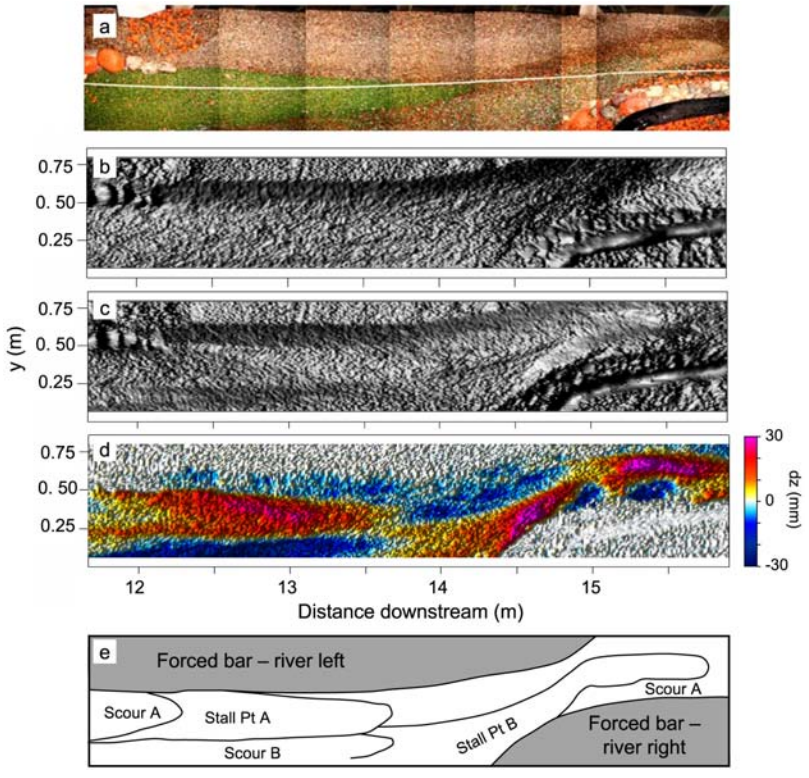

Figure 8. Reach-scale pulse progression through the channel. (a) The amalgamation of overhead photographs shows the leading edge of the pulse during the first large hydrograph. (b) Shaded relief map of topography before the first large hydrograph (run L18). (c) The topography corresponding to the photos in Figure 8a. (d) The change in elevation (*dz*) calculated by subtracting Figure 8c from Figure 8a. (e) Schematic of the process by which the pulse passes through the channel.

of the hydrograph (Figures 4c and 9c). The trailing edge of the pulse left the flume by the end of the second hydrograph. In contrast to the constant flow and small hydrograph runs, there is extensive erosion during the large hydrograph. This occurs because the flow depth was greatest during these runs, which increased the width of the bed load transport zone and resulted in the erosion of the original bar tails. These bars had been essentially behaving as abandoned terraces in the constant and small hydrograph runs. The addition of this eroded material likely contributed to the pulse progression rate.

4.3. Translation Versus Dispersion of Sediment Pulses

[44] The patterns of erosion and deposition in the channel provide some indication of how the pulse evolves, but in of themselves these observations are inadequate to assess the degree to which the pulse displays translation and dispersion. *Sklar et al.* [2009] presents a metric to aid in assessing whether a sediment pulse is translational or dispersive. In accordance with previous work [cf. *Lisle et al.*, 1997, 2001], they define a purely translational pulse as one where the leading and trailing edges, wave apex and center of mass, advance downstream and the pulse length remains the same. A purely dispersive sediment pulse is one where the wave apex and trailing edge do not migrate downstream and the pulse length grows. *Sklar et al.* [2009] note that these characteristics can be difficult to assess by simply looking at the elevation difference and recommend using the cumulative elevation difference (CED) curves normalized by the maximum CED. Figure 10 shows hypothetical CED curves for purely translational (Figure 10a), purely dispersive (Figure 10b), and mixed behavior (Figure 10c). For purely translational pulses, the slope of CED curves do not change and the leading and trailing edges move downstream. If there is no sediment supply from upstream, the total area under the curve remains constant as it moves downstream. The slope for a purely dispersive sediment pulse rotates about the origin in a clockwise direction.

[45] Here we use the CED curves for our sediment pulses to assess the relative importance of translation and dispersion. We calculate the elevation difference curve from a moving average longitudinal profile calculated from measured bed elevations following the method outlined by *Cui et al.* [2008]. The reach-averaged bed elevation is calculated at 0.01 m increments along the whole flume by averaging all laser scanned topographic points within a 4.3 m long window, 2.15 m upstream and 2.15 m downstream. This corresponds to a moving average over one wavelength of the forced pool-riffle sequence.

[46] The CED curves for the constant flow run (Figure 11a) show rotation of the slope about the sediment input location for the first three curves (t = 1:05, 3:13, 4:46) indicating dispersion. The measurement at t = 14:43 shows that the tail has moved downstream, but the slope of the

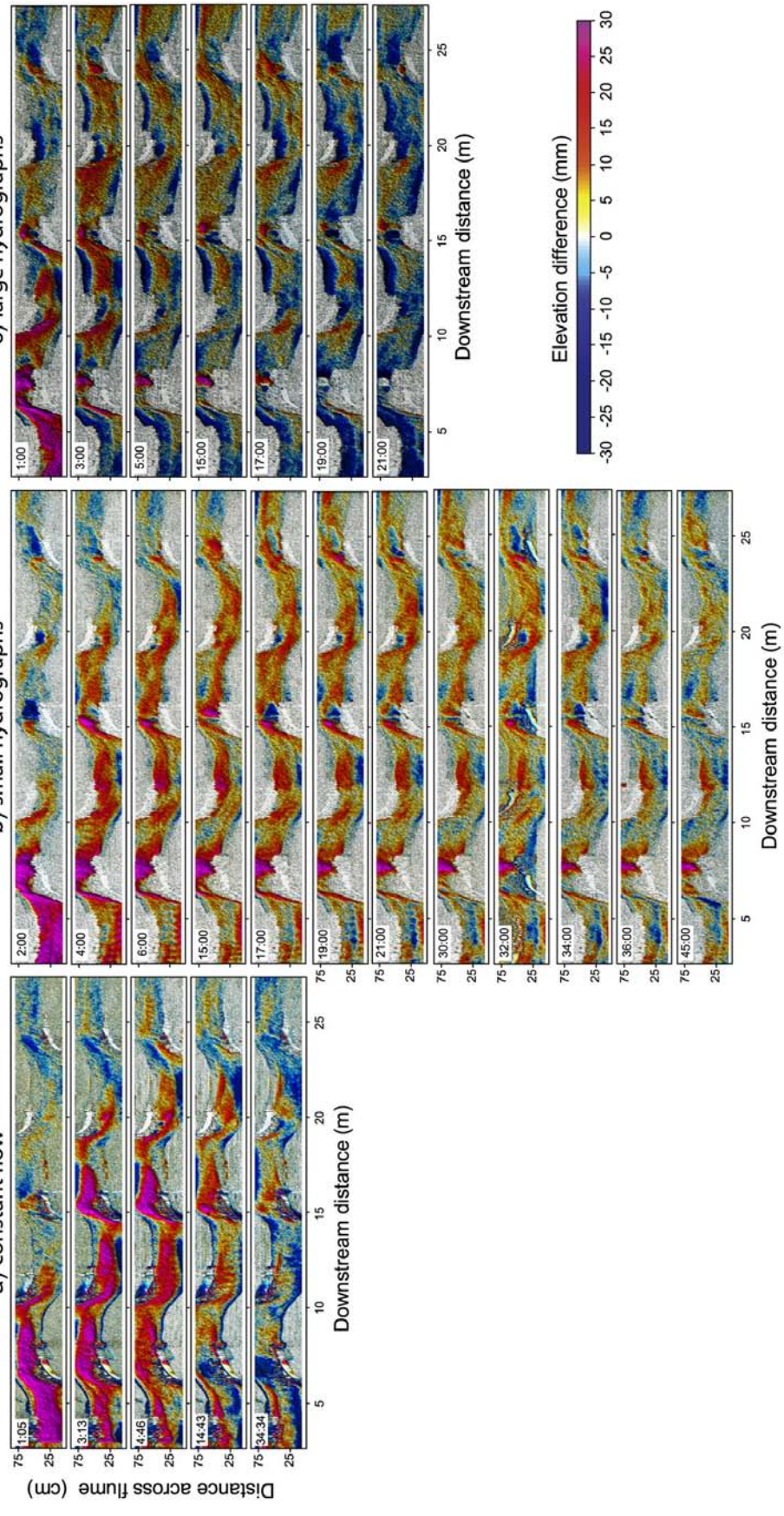

Figure 9. Maps of topographic change during (a) the constant flow, (b) small hydrograph, and (c) large hydrograph experiments. Experimental time is given in the top left corner of each panel. Topographic change is calculated by subtracting high-resolution laser bed surface scans from the prepulse topography. As such, elevation differences >0 indicate deposition, and values <0 indicate erosion.

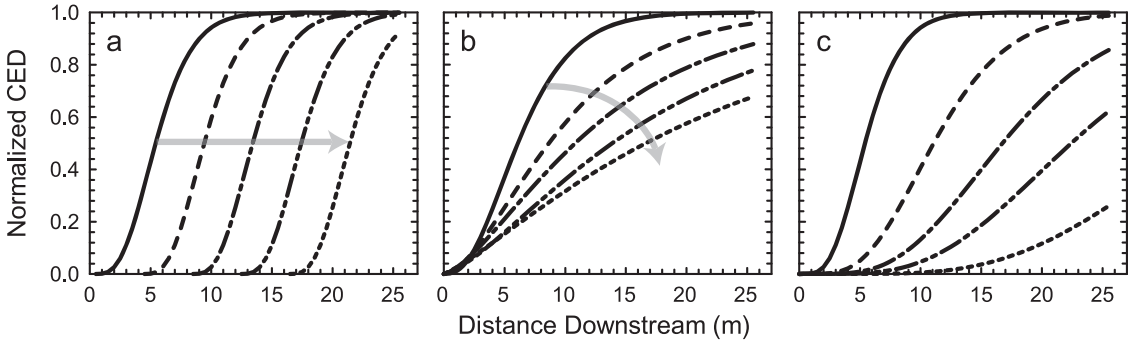

Figure 10. Cumulative elevation difference (CED) curves for hypothetical sediment pulses that (a) are purely translational, (b) are purely dispersive, and (c) have mixed behavior. The CED curves are the summation of all elevation differences moving downstream, normalized by the maximum cumulative elevation difference. See *Sklar et al.* [2009] for further details on how these curves were generated.

curve continues to decline suggesting a mixed behavior. By the end of the experiment at t = 34:39, the CED curve was negative because there was net erosion out of the flume.

[47] The CED curves for the three small hydrographs (Figure 11b) also show rotation of the slope about the sediment input location throughout the experiment. In contrast to the constant flow experiment, there is no movement of the tail suggesting the pulse is almost purely dispersive. An equivalent amount of water to the constant flow run was released by the end of the second hydrograph. Comparing the constant flow and small hydrograph CED curves indicate that far more material was moved out of the flume during the constant flow. Indeed, at the end of the third small hydrograph, there is still a large portion of the pulse material left within the flume. It is likely that one or two more hydrographs would be needed to complete the dispersion of the pulse material.

[48] The large hydrograph CED curves (Figure 11c) show rotation of the slope and progression of the tail along the zero change axis in the first 15 h of the run. This is indicative of a combination of translation and dispersion. The CED curve at 15 h is nearly identical to the curve at 5 h, indicating that the pulse does not move on the waning portion of the hydrograph. At the end of the first large hydrograph (t = 15 h), the pulse had almost entirely exited the flume, and by the end of the second large hydrograph (t = 30 h) there is no pulse material remaining in the flume. It is not possible to assess the degree of translation or dispersion using Figure 11c after the first hydrograph because the second hydrograph caused widespread scour of the bed and bar tails below the prepulse elevation.

5. Discussion

5.1. How Do Hydrographs Impact Sediment Transport?

[49] Temporal lags between flow and sediment transport are common. Peak wash load concentrations in rivers are often observed to occur before the peak in hydrographs, resulting in a clockwise hysteresis effect. This occurs because there is an abundant supply of fine sediment to the channel, deposited at low flow. This sediment is entrained on the rising limb of the hydrograph and then depleted

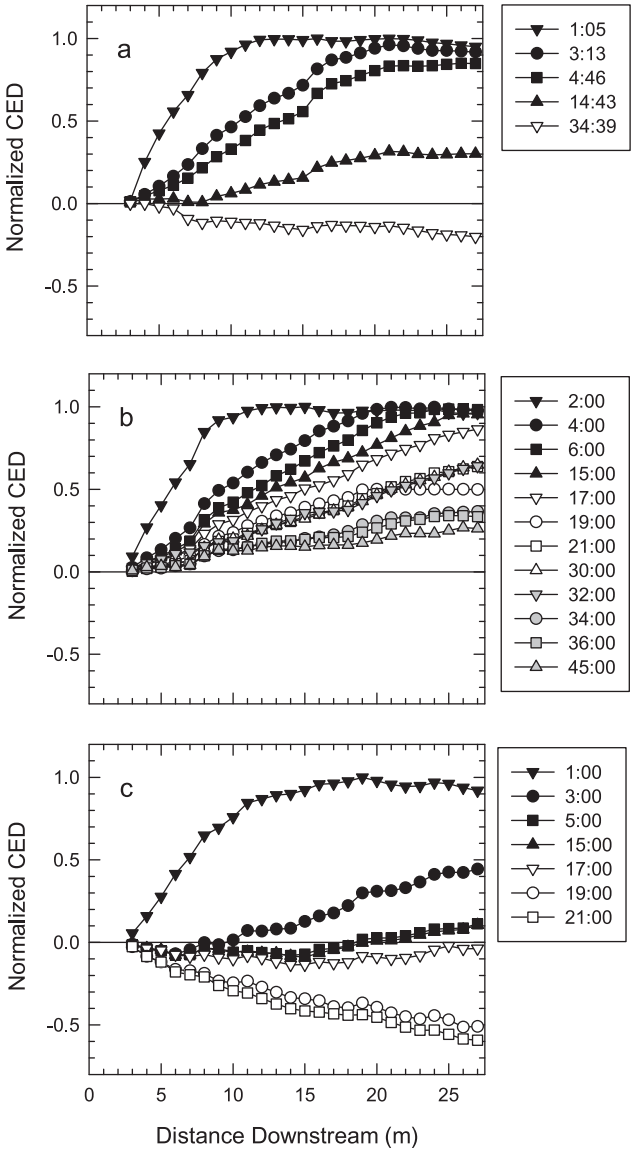

Figure 11. Elevation difference and cumulative elevation difference (CED) curves for (a) the constant flow, (b) the small hydrographs, and (c) the large hydrographs.

before the maximum flow occurs [*Church and Gilbert*, 1975; *Bogen*, 1980; *Walling and Webb*, 1987; *Asselman*, 1999]. Clockwise hysteresis can also happen when bed forms (ripples or dunes) are adjusted to long recessional flows but are deformed by rapidly rising flow and thus are out of phase with the flow, resulting in increased suspension [*Iseya*, 1982]. Counterclockwise hysteresis in wash load sediment transport is less commonly reported but can occur when sediment originates from a distant source [*Heidel*, 1956], when the valley slopes form the most important sediment source [*Walling et al.*, 1979; *Klein*, 1984], or because of bank failure after passage of a flood wave [*Ashbridge*, 1995].

[50] In contrast, bed load is commonly reported to lag behind changes in flow. This has been attributed to (1) bed form development lagging changes in flow [cf. *Neill*, 1969; *Griffiths and Sutherland*, 1977; *Bell and Sutherland*, 1983; *Lee et al.*, 2004], (2) the time necessary to destroy a well-established armor layer in gravel-bedded streams [*Kuhnle*, 1992], (3) differences in the entrainment probabilities between consolidated and loose beds [*Reid et al.*, 1985] or undisturbed and disturbed grains [*Jain*, 1992], (4) inertial properties of the bed [*Plate*, 1994; *Wang et al.*, 1994], (5) spatial lags where a finite length of the bed is needed to erode sufficient material to satisfy the transport capacity, in effect, a transport fetch length [*Bell and Sutherland*, 1983], (6) timing of sediment supply to the channel [*Habersack et al.*, 2001], and (7) the lag due to the transport distance between the source of bed load and the measurement point in a longitudinally patchy bed [*Lisle and Madej*, 1992].

[51] These lags between bed load and sediment transport can lead to complex hysteresis effects in gravel bed channels. *Kuhnle* [1992] reports that for hydrographs with high peak flows, there is a clockwise hysteresis effect (higher bed load transport rates on the rising limb than the falling limb), but the hysteresis is counterclockwise for hydrographs with lower peak flows. This is because the lower flows are unable to significantly alter the armor layer. At higher flows, the armor either disappears when the sediment supply rate approaches the transport capacity [*Dietrich et al.*, 1989] or the armor becomes mobile [*Andrews and Erman*, 1986; *Wilcock and DeTemple*, 2005]. *Kuhnle* [1992] reanalyzed experimental flume observations presented by *Griffiths and Sutherland* [1977] and found no hysteresis, despite a significant lag. However, sediment feed was adjusted to the transport capacity in their experiments.

[52] In our experiments we see both positive and negative lags that are linked to sediment supply to the channel. The peak in sediment flux lags the discharge peak (positive lag) during the hydrographs where the pulse was fed into the channel. However, the transport peak leads the discharge peak (negative lag) in subsequent hydrographs without the pulse feed (Figure 4 and Table 1). The positive lag observed during the first hydrograph in a series is caused by the time required for the pulse material to reach the end of the flume channel. The negative lag observed in subsequent hydrographs is caused by abundant sediment availability in the channel, which may derive from pool filling and scour, scour of the bar tails and bed (below the prepulse elevation) or the pulse exiting the channel during the rising limb. During the small hydrographs series, the pools fill with pulse sediment during the declining limb of the first hydrograph (Figure 9). The rising limbs of the subsequent hydrographs cause pools to scour, leading to the observed negative lag. During the first large hydrograph, pulse storage in the pools is minimal (Figure 9), however, the first hydrograph overtopped the terraced bars. This caused lateral erosion by destabilizing the bar slopes that then collapsed into the channel. This provided the channel with an increased sediment supply. The pulse begins leaving the channel during the rising limb of the first large hydrograph, which may also contribute to the negative lag.

[53] Regardless of the observed lag, transport rates in our experiments are much larger on the rising limb than on the falling limb, leading to a well-defined clockwise hysteresis in the relation between discharge and sediment transport (Figure 7). There are two reasons why this could occur in our experiments: size-selective transport and pool-scour and fill during the hydrograph. The changes in bed load grain size during a hydrograph suggest that size-selective transport is occurring in our experiments. The bed load coarsening on the rising limb and fining on the receding limb of the hydrographs that we observed (Figure 5) suggests that the bed surface is fining during the rising limb and coarsening on the receding limb. On the rising limb of the hydrographs, the proportion of the coarser grain sizes entrained from the bed and transported increases, which increases the overall transport rate. On the falling limb of the hydrograph, these larger particles are deposited and the overall transport rate declines. The clockwise hysteresis may also be related to pool scour and fill during the hydrograph. There is evidence in Figure 9 of scour in the pools adjacent to the bar heads on the rising limbs of the hydrographs (see hours 2, 17, and 32 in Figure 9b). On the falling limb of the hydrographs, these scour holes fill with sediment, limiting the amount of sediment exiting the pools, and ultimately reaching the end of the flume.

[54] It is intriguing to note that our observed sedigraph for the large hydrograph does not follow the predicted sedigraph on the receding limb of the hydrograph (Figure 4). There is little sediment exiting the flume after hour 5 of both large hydrographs, even though the flow is capable of moving particles. This may be due to some combination of bed coarsening and pool infilling on the recession limb or simply exhaustion of the available sediment. Our version of the *Wong and Parker* [2006b] relation is not size selective, so we cannot determine the relative impact of bed coarsening relative to pool infilling or sediment exhaustion on the transport rates.

[55] The deviation between the observed and predicted sedigraph is intriguing because it does not impact the cumulative transport during a hydrograph. A number of researchers have noted that bed load transport rates are essentially the same under steady and unsteady flows [*Griffiths and Sutherland*, 1977; *Bell and Sutherland*, 1983; *Phillips and Sutherland*, 1989, 1990; *Parker et al.*, 2007; *Wong and Parker*, 2006a]. Our results appear to confirm this idea. The increased transport rate that occurs on the rising limb of the hydrographs is compensated by a decline in the transport rate on the falling limb.

5.2. How Do Hydrographs Impact Pulse Movement?

[56] Gravel augmentations are designed to supply coarse material to channels where selective transport has created

armored, degraded, and immobile river beds. Gravel augmentations are typically designed to fine river beds and increase bed mobility in an effort to create conditions conducive to salmon spawning and rearing. There are two ways to achieve this goal. One way is to bury the coarse, degraded river bed with a desired grain size [cf. *Bunte*, 2004; *Harvey et al.*, 2005]. Another approach is to use a grain size much finer than the bed surface material to enhance mobility of the bed surface, revealing the subsurface material [*Venditti et al.*, 2010a]. Dispersion of pulse material is preferred when the existing bed material needs to be buried because it is too coarse to mobilize or where finer subsurface sediment deposits are thin or absent. Dispersion may also be preferred where a downstream sediment supply would be detrimental to ecological productivity or cause river bed level changes that could enhance flood risk. Some translation, in addition to dispersion may be the desired outcome when mobilization of a coarse surface layer is desired or where access points for sediment delivery are limited but a long downstream reach could potentially benefit from the added gravel [*Sklar et al.*, 2009; *Venditti et al.*, 2010a].

[57] Previous work has demonstrated that sediment pulses move by some combination of dispersion or translation, but that dispersion is by far the dominant progression pattern [*Lisle et al.*, 1997; *Cui et al.*, 2003b; *Lisle*, 2008]. However, most of this work has focused on natural sediment pulses formed by hillslope failure that often temporarily dam channels and have a sediment supply to the upstream side. Downstream of a dam, there is no sediment supply upstream of the augmentation site and pulses do not block the channel by design. Passive gravel augmentations are typically designed to feed sediment to downstream reaches, suggesting that they are low amplitude relative to the flow depth. In a synthesis of previous work, *Lisle* [2008] argues that these types of low-amplitude pulses and pulses composed of material finer than the prepulse bed material are more likely to exhibit some translation in addition to dispersion. The recent experimental work of *Sklar et al.* [2009] also shows that whether a gravel augmentation pulse translates or disperses is dependent on the pulse size and grain size.

[58] These experiments were designed explicitly to examine the effect of a hydrograph on pulse movement. By holding the pulse size and the total volume of water constant, we are able to determine how different types of hydrograph releases impact pulse translation and dispersion in a sediment-starved channel. Our results suggest that constant flows cause dispersion with some limited translation. The small hydrograph was dominated by dispersion and pulse sediments remained in the channel after the water was released. The large hydrograph showed a combination of dispersion and translation with most of the pulse sediment exiting the channel after the first hydrograph.

[59] The results suggest that selecting the type of flow release is critical to getting the desired results. Regardless of the specific translational or dispersive nature of our sediment pulses, it is clear from these experiments that a sediment pulse will persist in the channel for longer by releasing water in a series of small hydrographs than releasing the same volume of water in a constant flow. Our experiments suggest that using small hydrographs that peak at $\sim$2.5 times the threshold discharge for bed material entrainment and that have a long declining limb retained sediment for more than 1.5 times longer than the constant flow. Where some local downstream migration of the pulse sediment is desired, hydrographs with a peak $>$3 times the entrainment threshold discharge, with sharp declining limbs will move a sediment pulse out of the local reach more efficiently than a constant flow that exceeds the threshold for entrainment by $\sim$60%.

[60] An additional oft stated goal of gravel augmentations is to build topographic complexity (pools, bars, riffles). The movement of the pulses through the fixed alternate bar topography in our experiments suggests that sediment pulses could cause lateral channel migration. Regardless of the hydrograph type, pulse sediments stalled at the bar apex as they moved downstream. This deflected flow away from the bar apex toward the flume walls in our experiments. It is difficult to extrapolate this observation to a natural channel, but this deposition on the bar apex is akin to point bar growth that can result in lateral migration by a bar-push mechanism [*Johannesson and Parker* 1989] in a channel with fully mobile banks. In a stream restoration, this could be a potential benefit in that lateral channel activity is restored, which can result in greater channel complexity. This could also be a potential pitfall of gravel augmentation where channel migration by bar push mechanisms would impact streamside property.

6. Conclusions

[61] We conducted a series of experiments in a physical model of a river with a forced bar-pool morphology to study the effect of varying discharge on the passage of a gravel augmentation pulse in conditions indicative of a river downstream of a dam. A gravel augmentation pulse that is subjected to a hydrograph will not evolve in the same manner as one subjected to a constant flow rate. Complex topography has local reach-scale impacts on how sediment pulses move through channels. Pulse sediment tends to accumulate on point bars, which induces flow patterns that could cause lateral channel migration. As in previous work, hydrographs caused a clockwise hysteresis in sediment transport in our experiments. The way that water is released from a dam influences whether sediment pulse movement exhibits dispersion or a mixture of translation and dispersion. Large hydrographs with peak flows much greater than the entrainment threshold and steep rising and declining limbs cause some translation of sediment pulses, in addition to dispersion. Smaller hydrographs with peak flows $\sim$2.5 times greater than the entrainment threshold and gradual declining limbs cause dispersion of sediment pulses, without significant translation. Constant flows just above the threshold of motion tend to produce dispersion with some limited translation. Previous work has shown that river managers can choose a sediment pulse grain size and volume to optimize sediment transport conditions and pulse movement type (translation or dispersion). The ability to choose the hydrograph type to further optimize pulse movement provides river managers with an additional degree of freedom in designing gravel augmentations.

[62] **Acknowledgments.** Funding for this research was provided by CALFED Ecosystem Restoration Program (grant ERP-02D-P55), the National Center for Earth Surface Dynamics (NCED) under agreement EAR-0120914, and a NSERC Discovery grant to J.V. We are grateful to T.

Millet, T. Minear, J. Chayka, S. Foster, and J. Potter for laboratory assistance; C. Ellis, J. Mullin, B. Otteson, and C. Paola at St. Anthony Falls Laboratory, University of Minnesota for instrument cart development; P. Downs, S. Dusterhoff, C. Fixler, and F. Ligon of Stillwater Sciences for project management; and the project scientific advisory panel members T. Lisle, S. McBain, G. Parker, K. Vyverberg, and P. Wilcock for insightful discussions. W. E. Dietrich and Y. Cui helped us focus our experimental design.

References

Andrews, E. D. (2000), Bed material transport in the Virgin River, Utah, *Water Resour. Res.*, *36*(2), 585–596, doi:10.1029/1999WR900257.

Andrews, E. D., and D. C. Erman (1986), Persistence in the size distribution of surficial bed material during an extreme snowmelt flood, *Water Resour. Res.*, *22*(2), 191–197.

Ashbridge, D. (1995), Processes of river bank erosion and their contribution to the suspended sediment load of the River Culm, Devon, in *Sediment and Water Quality in River Catchments*, edited by I. D. L. Foster, A. M. Gurnell, and B. W. Webb, pp. 229–245, John Wiley, Chichester, U. K.

Asselman, N. E. M. (1999), Suspended sediment dynamics in a large drainage basin: The River Rhine, *Hydrol. Processes*, *13*, 1437–1450.

Bartley, R., and I. Rutherford (2005), Re-evaluation of the wave model as a tool for quantifying the geomorphic recovery potential of streams disturbed by sediment slugs, *Geomorphology*, *64*, 221–242, doi:10.1016/j.geomorph.2004.07.005.

Bell, R. G., and A. J. Sutherland (1983), Nonequilibrium bedload transport by steady flows, *J. Hydraul. Eng.*, *109*, 351–367.

Benda, L., and T. Dunne (1997a), Stochastic forcing of sediment supply to channel networks from landsliding and debris flow, *Water Resour. Res.*, *33*(12), 2849–2863, doi:10.1029/97WR02388.

Benda, L., and T. Dunne (1997b), Stochastic forcing of sediment routing and storage in channel networks, *Water Resour. Res.*, *33*, 2865–2880, doi:10.1029/97WR02387.

Bogen, J. (1980), The hysteresis effect of sediment transport systems, *Nor. Geogr. Tidsskr.*, *34*, 45–54.

Buffington, J. M., and D. R. Montgomery (1999), Effects of sediment supply on surface textures of gravel-bed rivers, *Water Resour. Res.*, *35*, 3523–3530.

Buffington, J. M., W. E. Dietrich, and J. W. Kirchner (1992), Friction angle measurements on a naturally formed gravel streambed: Implications for critical boundary shear stress, *Water Resour. Res.*, *28*, 411–425.

Bunte, K. (2004), Gravel mitigation and augmentation below hydroelectric dams: A geomorphological perspective, report, 144 pp., Stream Syst. Technol. Cent., Rocky Mtn. Res. Stn., For. Serv., U.S. Dep. of Agric., Fort Collins, Colo.

Church, M., and R. Gilbert (1975), Proglacial fluvial and lacustrine environments, glaciofluvial and glaciolacustrine sedimentation, *Spec. Publ. Soc. Econ. Paleontol. Minerol.*, *23*, 40–100.

Cui, Y., and G. Parker (2005), Numerical model of sediment pulses and supply disturbances in mountain rivers, *J. Hydraul. Eng.*, *131*, 646–656, doi:10.1061/(ASCE)0733-9429(2005)131:8(646).

Cui, Y., G. Parker, T. E. Lisle, J. Gott, M. E. Hansler-Ball, J. E. Pizzuto, N. E. Allmendinger, and J. M. Reed (2003a), Sediment pulses in mountain rivers: 1. Experiments, *Water Resour. Res.*, *39*(9), 1239, doi:10.1029/2002WR001803.

Cui, Y., G. Parker, J. Pizzuto, and T. E. Lisle (2003b), Sediment pulses in mountain rivers: 2. Comparison between experiments and numerical predictions, *Water Resour. Res.*, *39*(9), 1240, doi:10.1029/2002WR001805.

Cui, Y., J. Wooster, J. G. Venditti, S. Dusterhoff, W. E. Dietrich, and L. S. Sklar (2008), Simulating sediment transport in a highly two-dimensional flume: Examinations of two one-dimensional numerical models, *J. Hydraul. Eng.*, *134*, 892–904, doi:10.1061/(ASCE)0733-9429(2008)134:7(892).

Dietrich, W. E., J. W. Kirchner, H. Ikeda, and F. Iseya (1989), Sediment supply and the development of the coarse surface layer in gravel-bedded rivers, *Nature*, *340*, 215–217.

Folk, R. L., and W. C. Ward (1957), Brazos River bar: A study in the significance of grain size parameters, *J. Sediment. Petrol.*, *27*, 3–26.

Gilbert, G. K. (1917), Hydraulic mining debris in the Sierra Nevada, *U.S. Geol. Surv. Prof. Pap.*, *105*, 154 pp.

Griffiths, G. A., and A. J. Sutherland (1977), Bedload transport by translation waves, *J. Hydraul. Div. Am. Soc. Civ. Eng.*, *103*, 1279–1291.

Habersack, H. M., H. P. Nachtnebel, and J. B. Laronne (2001), The continuous measurement of bedload discharge in a large alpine gravel bed river, *J. Hydraul. Res.*, *39*, 125–133.

Harvey, B., S. McBain, D. Reiser, L. Rempel, L. S. Sklar, and R. Lave (2005), Key uncertainties in gravel augmentation: Geomorphological and biological research needs for effective river restoration, report, 99 pp., CALFED Sci. Program and Ecosyst. Restor. Program Gravel Augmentation Panel, Sacramento, Calif.

Heidel, S. G. (1956), The progressive lag of sediment concentration with flood waves, *Eos Trans. AGU*, *37*, 56–66.

Hoffman, D. F., and E. J. Gabet (2007), Effects of sediment pulses on channel morphology in a gravel-bed river, *Bull. Geol. Soc. Am.*, *119*, 116–125.

Iseya, F. (1982), A depositional process of reverse graded bedding in flood deposits of the Sakura River, Ibaraki Prefecture, Japan, *Geogr. Rev. Jpn.*, *55*, 597–613.

Jain, S. C. (1992), Note on lag in bedload discharge, *J. Hydraul. Eng.*, *118*(6), 904–917.

Johannesson, H., and G. Parker (1989), Linear theory of river meanders, in *River Meandering, Water Resour. Monogr. Ser.*, vol. 12, edited by S. Ikeda and G. Parker, pp. 181–213, AGU, Washington, D. C.

Kasai, M., T. Marutani, and G. J. Brierley (2004), Patterns of sediment slug translation and dispersion following typhoon-induced disturbance, Oyabu Creek, Kyushu, Japan, *Earth Surf. Processes Landforms*, *29*, 59–76, doi:10.1002/esp.1013.

Klein, M. (1984), Anti clockwise hysteresis in suspended sediment concentration during individual storms, *Catena*, *11*, 251–257.

Kondolf, G. M. (1997), Hungry water: Effects of dams and gravel mining on river channels, *Environ. Manage.*, *21*, 533–551.

Kuhnle, R. A. (1992), Bed load transport during rising and falling stages on two small streams, *Earth Surf. Processes Landforms*, *17*, 191–197.

Lee, K. T., Y.-L. Liu, and K.-H. Cheng (2004), Experimental investigation of bedload transport processes under unsteady flow conditions, *Hydrol. Processes*, *18*, 2439–2454.

Ligon, F. K., W. E. Dietrich, and W. J. Trush (1995), Downstream ecological effects of dams: A geomorphic perspective, *Bioscience*, *45*, 183–192.

Lisle, T. E. (2008), The evolution of sediment waves influenced by varying transport capacity in heterogeneous rivers, in *Gravel Bed Rivers VI: From Process Understanding to River Restoration*, edited by H. Habersack, H. Piegay, and M. Rinaldi, pp. 443–472, Elsevier, Amsterdam.

Lisle, T. E., and M. A. Madej (1992), Spatial variation in armouring in a channel with high sediment supply, in *Dynamics of Gravel-Bed Rivers*, edited by R. D. H. P. Billi, C. R. Thorne, and P. Tacconi, pp. 277–291, John Wiley, Chichester, U. K.

Lisle, T. E., J. E. Pizzuto, H. Ikeda, F. Iseya, and Y. Kodama (1997), Evolution of a sediment wave in an experimental channel, *Water Resour. Res.*, *33*, 1971–1981, doi:10.1029/97WR01180.

Lisle, T. E., Y. Cui, G. Parker, J. E. Pizzuto, and A. M. Dodd (2001), The dominance of dispersion in the evolution of bed material waves in gravel-bed rivers, *Earth Surf. Processes Landforms*, *26*, 1409–1420,

Lutrick, E. (2001), A review of gravel addition projects on Clear Creek, the Tuolumne River and the Stanislaus River, California: Implications for CALFED Bay-Delta program project management, M.S. thesis, 64 pp., Dep. of Landscape Archit. and Environ. Planning, Univ. of Calif., Berkeley.

Madej, M. A. (2001), Development of channel organization and roughness following sediment pulses in single-thread, gravel bed rivers, *Water Resour. Res.*, *37*, 2259–2272.

Neill, C. R. (1969), Bed Forms of the Lower Red Deer River, Alberta, *Journal of Hydrology*, *7*(1), p. 58–85.

Parker, G., M. A. Hassan, and P. Wilcock (2007), Adjustment of the bed surface size distribution of gravel-bed rivers in response to cycled hydrographs, in *Gravel-Bed Rivers VI: From Process Understanding to River Restoration*, edited by H. Habersack, H. Piegay, and M. Rinaldi, pp. 241–290, Elsevier, Amsterdam.

Pasternack, G. B., C. L. Wang, and J. E. Merz (2004), Application of a 2D hydrodynamic model to design of reach-scale spawning gravel replenishment on the Mokelumne River, California, *River Res. Appl.*, *20*, 205–225.

Phillips, B. C., and A. J. Sutherland (1989), Spatial lag effects in bed load sediment transport, *J. Hydraul. Res.*, *27*, 115–133.

Phillips, B. C., and A. J. Sutherland (1990), Temporal lag effects in bed load sediment transport, *J. Hydraul. Res.*, *28*, 5–23.

Pickup, G., R. J. Higgins, and I. Grant (1983), Modeling sediment transport as a moving wave—The transfer and deposition of mining waste, *J. Hydrol.*, *60*, 281–301, doi:10.1016/0022-1694(83)90027-6.

Plate, E. J. (1994), The need to consider non-stationary sediment transport, *Int. J. Sediment Res.*, *9*, 117–123.

Reid, I., L. E. Frostick, and J. T. Layman (1985), The incidence and nature of bedload transport during flood flows in coarse-grained alluvial channels, *Earth Surf. Processes Landforms*, *10*, 33–44.

Sklar, L. S., J. Fadde, J. G. Venditti, P. Nelson, M. A. Wydzga, Y. Cui, and W. E. Dietrich (2009), Translation and dispersion of sediment pulses in flume experiments simulating gravel augmentation below dams, *Water Resour. Res.*, *45*, W08439, doi:10.1029/2008WR007346.

Sutherland, D. G., M. Hansler Ball, S. J. Hilton, and T. E. Lisle (2002), Evolution of a landslide-induced sediment wave in the Navarro River, California, *Geol. Soc. Am. Bull.*, *114*, 1036–1048, doi:10.1130/0016-7606(2002)114<1036:EOALIS>2.0.CO;2.

Venditti, J. G., W. E. Dietrich, P. A. Nelson, M. A. Wydzga, J. Fadde, and L. Sklar (2010a), Effect of sediment pulse grain size on sediment transport rates and bed mobility in gravel bed rivers, *J. Geophys. Res.*, *115*, F03039, doi:10.1029/2009JF001418.

Venditti, J. G., W. E. Dietrich, P. A. Nelson, M. A. Wydzga, J. Fadde, and L. Sklar (2010b), Mobilization of coarse surface layers in gravel-bedded rivers by finer gravel bed load, *Water Resour. Res.*, *46*, W07506, doi:10.1029/2009WR008329.

Walling, D. E., and B. W. Webb (1987), Suspended load in gravel-bed rivers: UK experience, in *Sediment Transport in Gravel-Bed Rivers*, edited by C. R. Thorne, J. C. Bathurst, and R. D. Hey, pp. 691–732, John Wiley, New York.

Walling, D. E., M. R. Peart, F. Oldfield, and R. Thompson (1979), Suspended sediment sources identified by magnetic measurements, *Nature*, *281*, 110–113.

Wang, Z., W. Kron, and E. J. Plate (1994), An experimental study of bed deformation in unsteady and non-uniform flows, *Int. J. Sediment Res.*, *9*, 206–215.

Wilcock, P. R., and B. T. DeTemple (2005), Persistence of armor layers in gravel-bed streams, *Geophys. Res. Lett.*, *32*, L08402, doi:10.1029/2004GL021772.

Wohl, E., P. L. Angermeier, B. Bledsoe, G. M. Kondolf, L. MacDonnell, D. M. Merritt, M. A. Palmer, N. L. Poff, and D. Tarboton (2005), River restoration, *Water Resour. Res.*, *41*, W10301, doi:10.1029/2005WR003985.

Wong, M., and G. Parker (2006a), One-dimensional modeling of bed evolution in a gravel bed river subject to a cycled flood hydrograph, *J. Geophys. Res.*, *111*, F03018, doi:10.1029/2006JF000478.

Wong, M., and G. Parker (2006b), Reanalysis and correction of bed-load relation of Meyer-Peter and Muller using their own database, *J. Hydraul. Eng.*, *132*, 1159–1168, doi:10.1061/(ASCE)0733-9429(2006)132:11(1159).

Wooster, J. K., S. R. Dusterhoff, Y. Cui, L. S. Sklar, W. E. Dietrich, and M. Malko (2008), Sediment supply and relative size distribution effects on fine sediment infiltration into immobile gravels, *Water Resour. Res.*, *44*, W03424, doi:10.1029/2006WR005815.

R. Humphries and J. G. Venditti, Department of Geography, Simon Fraser University, Burnaby, BC V5A 1S6, Canada. (jeremy_venditti@sfu.ca)

L. S. Sklar, Department of Geosciences, San Francisco State University, San Francisco, CA 94132, USA.

J. K. Wooster, Habitat Conversation Division, National Marine Fisheries Service, National Oceanic and Atmospheric Administration, 650 Capital Mall, Suite 5-100, Sacramento, CA 95814-4708, USA.